Studii şi Cercetări Ştiinţifice 2016, **17** (2), pp. 125 – 137
Chimie şi Inginerie Chimică, Biotehnologii, Industrie Alimentară

Scientific Study & Research
Chemistry & Chemical Engineering, Biotechnology, Food Industry *ISSN 1582-540X*

ORIGINAL RESEARCH PAPER

FLUX PROFILES AND MATHEMATICAL MODELING OF FOULING MECHANISM FOR ULTRAFILTRATION OF KONJAC GLUCOMANNAN

Nita Aryanti[1*], Dyah H. Wardhani[1], Supandi Supandi[2]

[1]Diponegoro University, Department of Chemical Engineering, Kampus Undip Tembalang, Semarang, Indonesia
[2]Universitas PGRI Semarang, Department of Mathematics Education, Faculty of Mathematics, Science and Information Technology, Jl. Sidodadi Timur no 24, Semarang, Indonesia

*Corresponding author: nita.aryanti@che.undip.ac.id

Received: February, 25, 2016
Accepted: May, 27, 2016

Abstract: This study was focused on principles and fouling analysis of konjac glucomannan (KGM) separation using ultrafiltration system. Two Polyethersulfone membranes (PES) having molecular weight cut-off of 10 and 20 kDa were used. It was found that membrane having larger pore size provided higher flux profiles. Evaluation of different transmembrane pressures resulted on possibility of more severe fouling at higher membrane pressure. With the increase of konjac glucomannan concentration, decrease of profile flux was observed. Further, a simple mathematical modelling of fouling mechanism was analyzed based on Hermia's model. The images of membrane surfaces and cross-sections obtained by scanning electron microscopy (SEM) were examined and being compared with the model. The research found that the fouling mechanisms of KGM ultrafiltration using membrane with pore size of 10 kDa was complete blocking. On the contrary, cake/gel layer formation was a fouling mechanism for ultrafiltration system with pore size of 20kDa.

Keywords: *konjac glucomannan, ultrafiltration, polyethersulfone membranes, fouling mechanism, mathematical modelling*

INTRODUCTION

Konjac (*Amorphophallus konjac*) is a carbohydrate rich plants containing glucomannan, a polysaccharide consisting of D-mannose and D-glucose monomers with β (1 - 4) linkage [1]. One of the konjac species is *Amorphophallus onchophyllus*, known as porang which has been cultivated in forest border around Central and East Java, Indonesia. Konjac glucomannan (KGM) and its derivatives have been applied for various fields such as food additives, drug delivery, bioadhesive improvement, immobilization, encapsulation, film and membranes, coating as well as emulsifier and surfactant [1, 2]. Extraction and purification of KGM from konjac tuber require complex processes [3, 4]. The purification of KGM plays an important role in improving KGM quality. Some methods use multistage dialysis or centrifugation [3, 5].
Alternatively, ultrafiltration system (UF) has been identified as a well-established separation process in industry. Ultrafiltration is a low-pressure membrane filtration process which operates between pressures of 1 to 10 bar [6]. The pore sizes in UF membranes range from 0.002 μm to 0.2 μm, which result in rejections of compounds in the molecular weight range from 1000 to 100000 Daltons. Ultrafiltration requires pressure as driving force to filter the solution through the membrane and to separate solutes from the solution based membrane's molecular weight cut-off. There are no changes of phase or state during the ultrafiltration process and the solute separate at room temperature. This make the ultrafiltration process requires less energy compared to conventional process [6]. This membrane is capable for separating polysaccharides from co-extracted molecules [7], isolation of hemicellulose [8] as well as fractionation of polysaccharides from rapeseed [9] and sweet tea extract [10]. As a glucomannan is a polysaccharide, it is certain of that ultrafiltration is competent to separate and purify the KGM.
However, research focused on glucomannan separation using ultrafiltration was very limited. Jian et al. [11] studied the preparation and separation of Konjac oligosaccharides. First, the konjac glucomannan was degraded by the combination of γ-irradiation and β-mannase, and then ultrafiltration was used to separate degradation product. In membrane technology, the polysaccharide such as glucomannan is potential material causing membrane fouling. Hence, a comprehensive analysis of konjac glucomannan fouling is significant for investigation of KGM Ultrafiltration. Since evaluation of membrane fouling by KGM solution is not available, this research is focused on ultrafiltration of KGM solution. More specific, performance of ultrafiltration for KGM separation was examined as well as study on fouling mechanism. This research is very significant since fouling mechanism will contribute to suitable membrane cleaning.
Mathematical modelling of fouling mechanism of the KGM ultrafiltration was studied based on Hermia's model. This model has been applied for fouling mechanism evaluation of many separation processes using ultrafiltration such as whey model solution [12], skimmed coconut milk [13], extract of traditional Chinese medicine [14] and extracelullar polymeric substances [15]. The Hermia's model describes mechanism of membrane fouling based on blocking filtration law, consisting of complete pore blocking, standard pore blocking and intermediate pore blocking and cake filtration. The blocking law filtration is expressed in the term of permeate time and filtration time and developed for dead-end filtration as shown in eqn. (1) [16, 17]:

$$\frac{d^2t}{dV^2} = k\left(\frac{dt}{dV}\right)^n \tag{1}$$

where t is filtration time and V is the permeate volume, k is constant and n is a value illustrating the different fouling mechanism.

The values of n are described as follow: complete blocking having n value of 2, intermediate blocking is represented with n = 1, the standard blocking illustrated with n = 1.5 and the cake layer formation has n value of 0. In the complete blocking model, it is assumed that each solute participated in blocking completely the entrance of the membrane pores. For intermediate blocking, it is assumed that every solute is stayed on previously deposited solute. Standard blocking considers the deposition of each solute to the internal pore wall. The cake layer formation applied based on the accumulation of the solute on the membrane surface in the cake form [18].

The Hermia's model were then linearized based on the n value for each model using fitting equation in terms of permeate flux versus time as presented in eqn. (2) to eqn. (5).

For Complete Blocking (n = 2):

$$\ln J = \ln J_0 - k_c t \tag{2}$$

For Intermediate Blocking (n = 1):

$$\frac{1}{J} = \frac{1}{J_0} + k_i t \tag{3}$$

For Standard Blocking (n = 1.5):

$$\frac{1}{\sqrt{J}} = \frac{1}{\sqrt{J_0}} + k_s t \tag{4}$$

For Cake/Layer Formation (n = 0):

$$\frac{1}{J^2} = \frac{1}{J_0^2} + k_{cf} t \tag{5}$$

where k_c, k_i, k_s and k_{cf} are constants for complete blocking, intermediate blocking and cake/layer formation, respectively.

MATERIALS AND METHODS

Konjac glucomanan (KGM) characterization

Glucomannan solution was prepared by mixing purified konjac glucomannan (New Foods, USA) with distilled water. The concentration of KGM in the solution was 1.5 g·L^{-1} and 5 g·L^{-1}. The molecular weight of KGM was not determined, however, data showed that commercial KGM have molecular weights of 2.56 × 10^5-1.57 × 10^6 Da [4, 19]. Based on the particle size analysis of KGM microscopy image, it was found that

the KGM had particle sizes of 100 - 210 μm which were similar to other data, 110 - 280 μm [3].

Membrane characterization

The morphology and structural changes of unused membrane and fouled membrane were visualized by an Inspect S50-FEI Scanning Electron Microscope (SEM) at various magnifications. The unused and fouled membrane was dried before analysis. The membrane surface and cross-sectional microscopic views were observed to compare the structural and morphology changes between unused and fouled membranes.

Ultrafiltration

Two commercial Polyethersulfone membranes (PES) having pore diameter of 10 kDa and 20 kDa obtained from Sepro, CA and Alfa-Laval Denmark, respectively, were used. The membranes were a round flat membrane polyethersulfone membranes (PES) membrane with a surface area of 0.00138 m^2. An ultrafiltration cell of 500 mL capacity was used for experimental works. Schematic diagram of the experimental apparatus is shown in Figure 1.

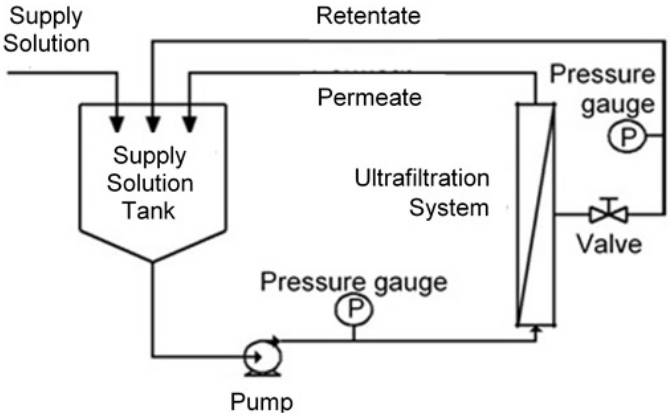

Figure 1. *Schematic illustration of ultrafiltration unit*

Before starting the experiments, the membranes were soaked in distilled water for about 12 hours. Then the membrane was compacted by filtering water for 30 minutes. The initial water flux (J_0) was obtained by measuring the volume of permeate water collected at specific recorded time. In order to evaluate the membrane fouling the ultrafiltration apparatus was operated by filtering KGM solution in a dead end mode, at ambient temperature (23 – 25 °C) and 1 - 3 bar operating pressure. The filtrations were carried out at total recycle mode where both permeate and retentate were recycled to the supply solution tank for maintaining same concentration. The permeate fluxes (J) were obtained by measuring volume of permeate collected at 5 minutes intervals for 120 minutes and were calculated using eqn. (6):

$$J = \frac{Q}{(A.t)} \qquad (6)$$

where: J: flux ($L \cdot m^{-2} \cdot h^{-1}$), Q: volume (L), A: membrane area (m^2) and t: time interval (h).

After each flux determination, the collected permeate was returned back to the supply solution tank. Further, normalized fluxes are obtained by dividing fluxes (J) with initial water fluxes (J_0).

RESULT AND DISCUSSION

Water flux characteristic

In order to identify the characteristics of separation of the membrane used, hydraulic permeability was measured. Water flux as a function of transmembrane pressure (TMP) for PES 10 and 20 kDa is shown in Figure 2.

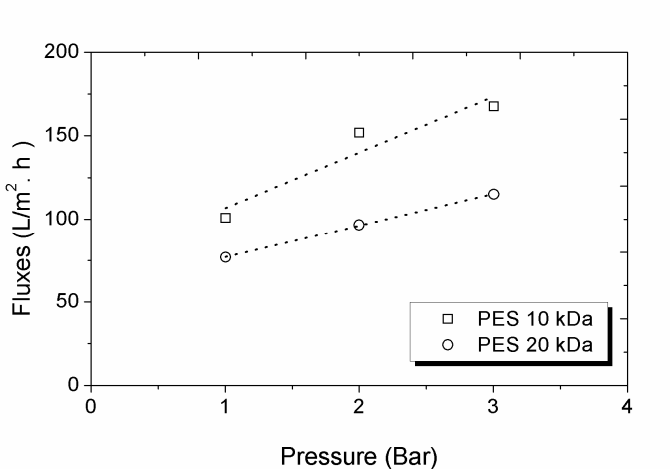

Figure 2. *Water flux as a function of trans membrane pressure for different membrane used*

Water fluxes were increased with the increase of pressure. It was found that a linear water flux increase with pressure regardless of the membrane molecular weight cut-off and type of membrane used [20]. For a membrane with uniform pore size, an idealized water flux versus pressure curve exhibited linear change [21]. It can be seen that for all transmembrane pressure, the water flux for PES 10 kDa membrane was higher than the water flux for PES 20 kDa membrane. The membrane permeability were 18.63 $L \cdot m^{-2} \cdot bar^{-1}$ and 33.395 $L \cdot m^{-2} \cdot bar^{-1}$ for PES 20 kDa and PES 10kDa, respectively. The result was in contradiction with those found by Wan et al. [22]. This is very interesting that the membrane with bigger molecular weight cut off typically having higher flux. Wang et al. [23] have observed similar phenomenon and it was found that it was due to different fouling mechanism. However, the explanation was not suitable for this experiment (see section **Mathematical model of fouling mechanism**).
The cross-sectional microscopy images of unused membrane (Figure 3) were then evaluated in order to explain the difference.

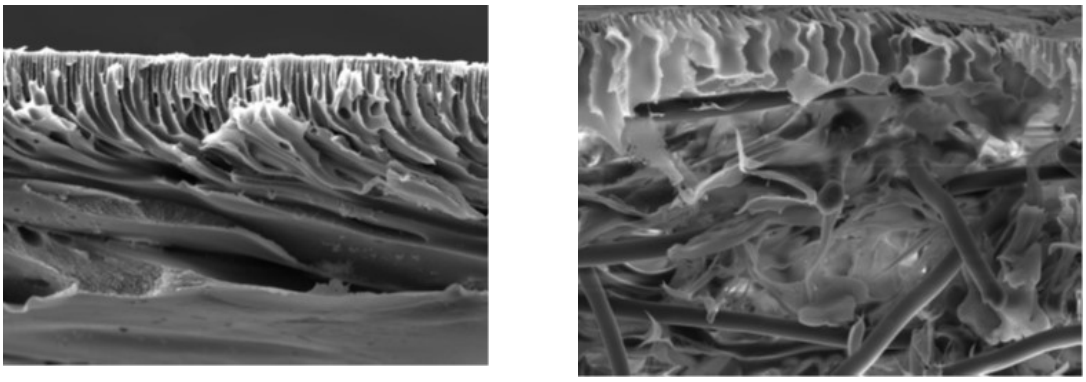

(a) ***(b)***

Figure 3. *Cross-sectional microscopy images of unused membrane (a) PES 10kDa (b) PES 20 kDa (SEM with 1000x magnification)*

Figure 3a depicted that the PES 10 kDa consist only interpore structure with continuous pore opening. On the contrary, on Figure 3b, the PES 20 kDa not only having the interpore structure but also supporting material. The interpore structure of the PES 20 kDa was shorter than the PES 10 kDa. In addition, the supporting material provides additional resistance in the membrane and affecting the water flux and permeability.

Effect of Membrane's Molecular Weight Cut-Off on Flux Profiles

The performance of the two PES membranes with nominal pore size of 10 kDa and 20 kDa was investigated (Figure 4). The transmembrane pressure was 1 bar and the initial KGM concentration was 1.5 $g \cdot L^{-1}$.

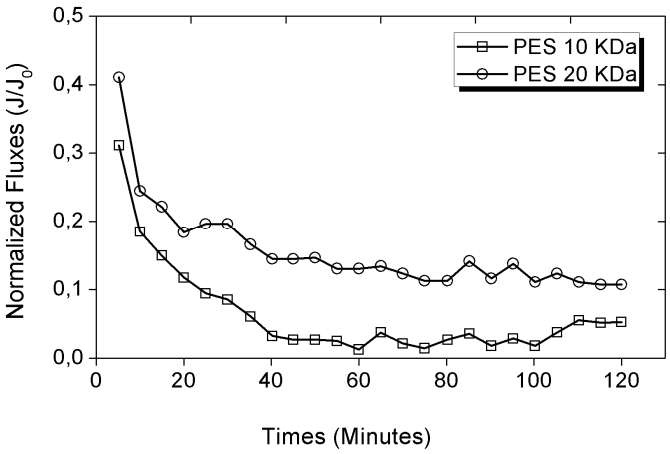

Figure 4. *Normalized flux profile during ultrafiltration of KGM (PES 10 kDa and 20 kDa at pressure of 1 bar and KGM concentration on supply solution of 1.5 $g \cdot L^{-1}$)*

In the ultrafiltration process, the permeate flux was lower for the KGM solution than for pure water due to severe concentration polarization caused by KGM molecules. The permeate flux decreased rapidly after 20 minutes of ultrafiltration. The higher normalized flux decline was found for PES 10 kDa than PES 20 kDa. This result was in contradiction compared to the water flux (Figure 2). If the size of separated particle is

the same order of magnitude, the smaller pore size membrane will result in higher flux [6]. The larger membrane pores will plug up first and hence the membrane will foul rapidly. Wang et al. [23] reported that pore size of membrane had influence over fouling mechanism. It was found that different fouling mechanism caused the flux phenomenon was unlike. When the mechanism is cake/gel formation and the gel is easily removed than the membrane flux was greater than those controlled by pore blocking. This explanation is further examined and the results are found in analysis of Hermia's model on the following section.

Effect of membrane's transmembrane pressure on flux profiles

Ultrafiltration for process separation is driven by transmembrane pressure (TMP). To investigate the effects of TMP on fouling behavior, the UF experiment of solution containing 1.5 $g \cdot L^{-1}$ of KGM was performed at different TMPs (1.2 and 3 bar) using the PES 20 kDa membrane as shown in Figure 5.

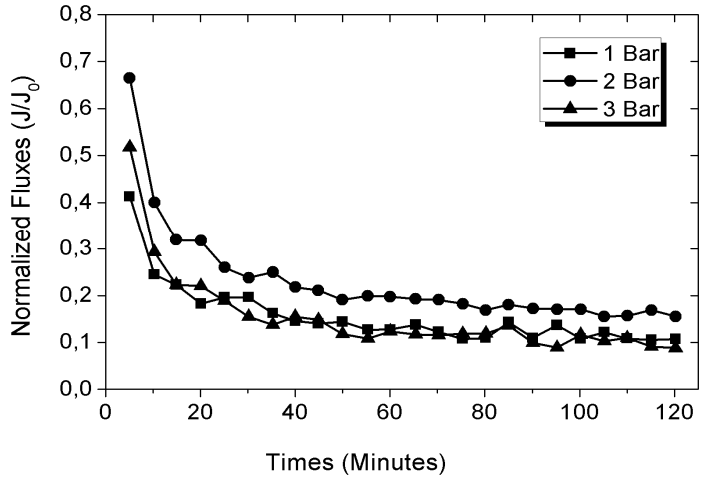

Figure 5. *Normalized flux profile during ultrafiltration of 1.5 $g \cdot L^{-1}$ KGM using PES 20 kDa at various transmembrane pressure (TMP)*

Figure 5 presented that higher TMP yielding of higher normalized flux (from 1 - 2 bar). However, when the TMP was increased to 3 bar, the normalized flux decreased, even though the normalized flux for 3 bar is higher than the 1 bar's flux in the beginning of operation. The amounts of solute at the membrane surface as well as in the membrane pore increases with the increase of TMP as a consequence of the increase of permeate fluxes. This can further promote adsorption of solute on/in the membrane and hence leading to adsorptive fouling. In addition, the increase of solute concentration at the membrane surface increases osmotic pressure effect, which will reduce the permeate flux [24].

It was also reported that the permeate flux proportionally increased at a low membrane pressure condition when operating pressure reached a critical value of the flux decreased [25]. In addition, the membrane permeation rate was reduced by the formation of a polarization layer on the membrane during membrane filtration [26]. The fouling layer on the membrane that resulted from deposition and accumulation of

solution particle became compacted at a higher pressure condition than at a lower pressure condition [6, 22, 27]. Moreover, it can be pronounced that at 1 - 2 bar, the ultrafiltration is affected by the membrane pressure (pressure controlled region) and at 3 bar is controlled by mass transfer [6].

Effect of KGM concentration on flux profiles

Supply solution concentration is one of major parameter affecting the permeate flux [6]. In order to evaluate initial concentration of supply solution influencing on the ultrafiltration performance, the supply solution containing different concentration of KGM were prepared and ultrafiltered using 20 kDa membrane. The applied pressure for this experiment was 1bar. Ultrafiltration tests were carried out with KGM concentration of 1.5 and 5 $g \cdot L^{-1}$. Figure 6 depicted the effect of KGM concentration on normalized flux.

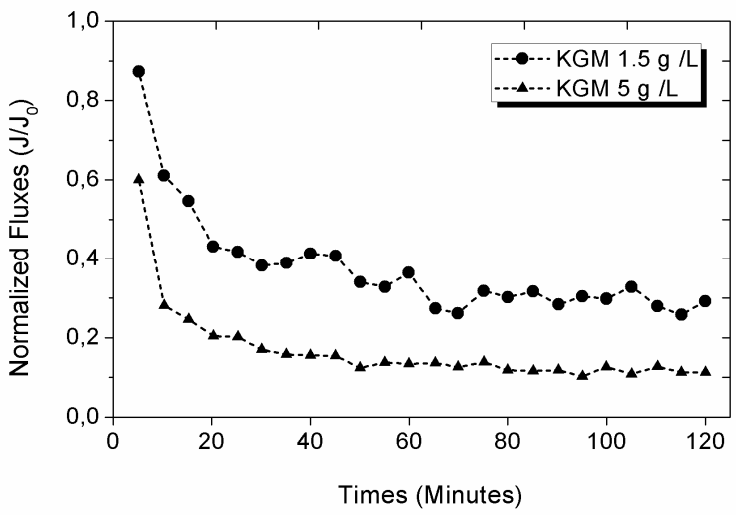

Figure 6. *Normalized flux profiles for different KGM concentration of supply solution at a pressure of 1 bar using the 20 kDa PES membrane*

The figure clearly shown that initial concentration of KGM in UF supply solution influenced permeate flux behaviour. A sharp decrease in flux is also observed. The supply solution containing higher concentration of KGM results on higher permeate flux decline. In addition, it is predicted that solute concentration at the membrane surface is greater for the higher supply solution concentration. As a consequences, the adsorptive fouling and cake layer formation were promoted leading to more severe fouling [26]. This fact can also be attributed due to the phenomenon called concentration polarization, i.e. cake layer formation. The cake layer formation is more probable to be formed when working with highly concentrated solutions. Hence, the more concentrated solutions, the more pronounced decay in the permeate fluxes [28]. At higher concentration of KGM as a polysaccharide, the combination of cake formation and pore constriction was observed. In contrast, at lower concentration of polysaccharides, cake formation was found to be the dominant fouling mechanism [15].

Mathematical model of fouling mechanism

Hermia's model was applied in order to understand the membrane fouling during ultrafiltration of KGM. By fitting the experimental data into the Hermia's linearized equation (eqn. (2) to eqn. (5)), mechanism prevailing the fouling can be identified. Figure 7 showed the fitting experimental data to four types of Hermia's model. Table 1 showed all the corresponding correlation coefficients (R^2), and the bold maximal R^2 value indicating the best fitting model.

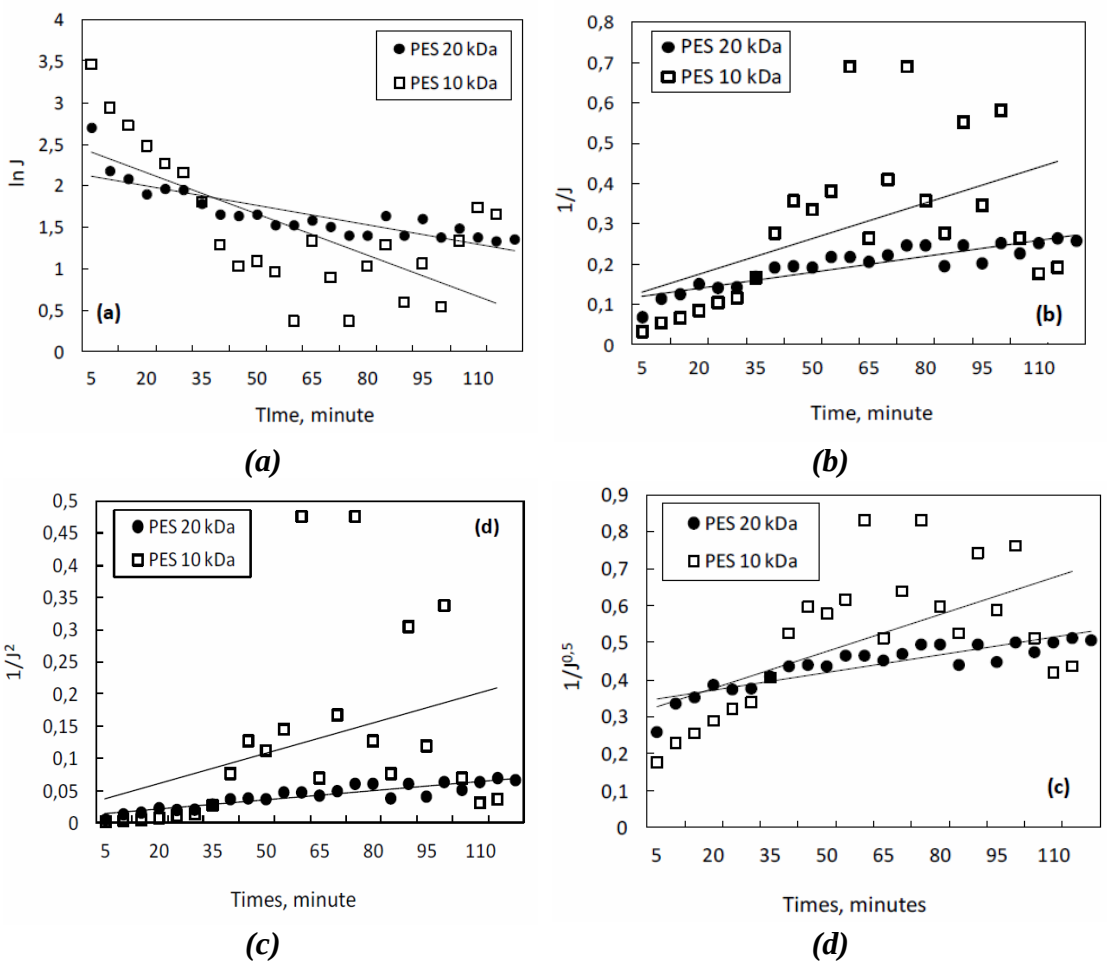

Figure 2. *Fitting of experimental data to Hermia's model: (a) complete blocking (b) intermediate blocking (c) standard blocking (d) cake/gel layer formation*

Table 1. *Measure of fitting experimental data to Hermia's model linear equations*

Membrane	R^2 Value			
	Complete	Intermediate	Standard	Gel/Cake Layer
PES 10 kDa	**0.4434**	0.2658	0.359	0.1388
PES 20 kDa	0.7127	0.8101	0.7736	**0.8372**

It can be seen in Figure 7 that PES 20 kDa membrane seems fit to all fouling mechanism. On the contrary, the PES 10 kDa membrane did not match to any fouling

mechanism. To find the best fit model of both membranes, the corresponding coefficients were evaluated (Table 1). Based on Table 1, it was obvious that the PES 10 kDa membrane is fit with the complete blocking model and the PES 20 kDa membrane is suitable for Cake/Gel layer formation model.

The complete blocking model leads to accumulation of particles/solutes on the membrane surface [23] but the particles do not overlap to other solute that has previously deposited on the membrane surface [18]. The cake/gel layer formation impedes the entrance molecules into the membrane pore and keeps them back on the cake layer. If the cake layer has a relatively loosen structure, the membrane flux can be higher than complete blocking model [23]. This gives additional explanation why the PES 20 kDa obtain higher flux than the PES 10 kDa. In the cake layer formation and complete blocking, both indicate that the KGM particle were much greater than the membrane pore size. The particles were accumulated on the membrane surface and blocked the membrane pores. The microscopy images of PES 20 kDa surface (Figure 8) give the evidence. However, eventhough the PES 20 kDa having cake/gel layer formation fouling mechanism, its permeate flux was higher than the PES 10 kDa. This is due to the fact that the cake layer fouling can be easily removed by water flushing than complete blocking model [23].

Surface and cross-sectional membrane analysis

Scanning electron microscopy images of the membrane sample (PES 20 kDa) is shown in Figure 8a and 8b for surface and cross-sectional view, respectively.

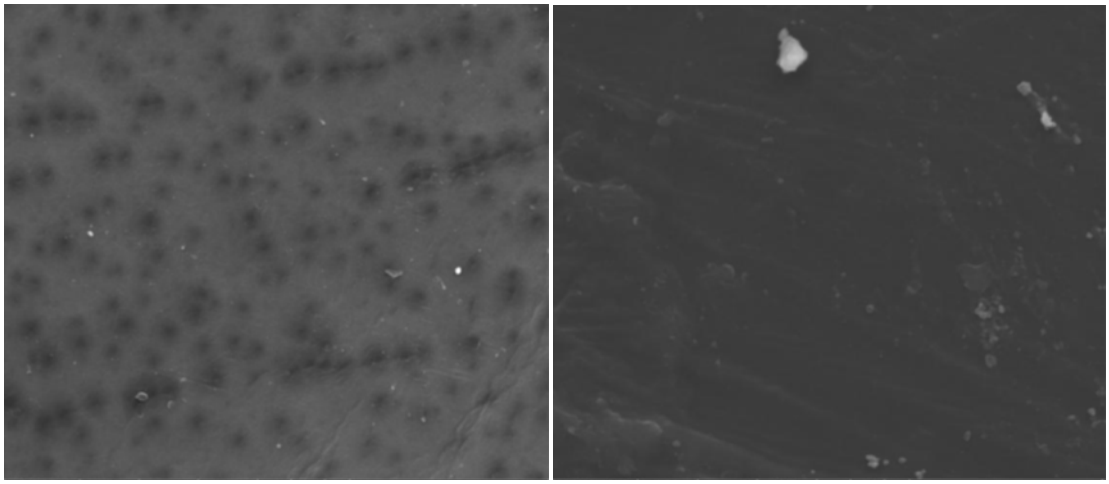

(a) ***(b)***

Figure 8. *Surface microscopy images of 20 kDa PES membrane : (a) unused membrane (b) fouled membrane by UF of 1.5 g·L^{-1} KGM (10.000 x magnification)*

The surface of unused membrane (Figure 8a) indicated top surface with clear pore opening. In contrast to Figure 8b for the fouled membrane, the microscopy image clearly indicates no pore opening on the membrane surface due to a layer covering the membrane surface.

Figure 9 displayed cross-sectional view of unused and fouled membrane when applied for KGM separation.

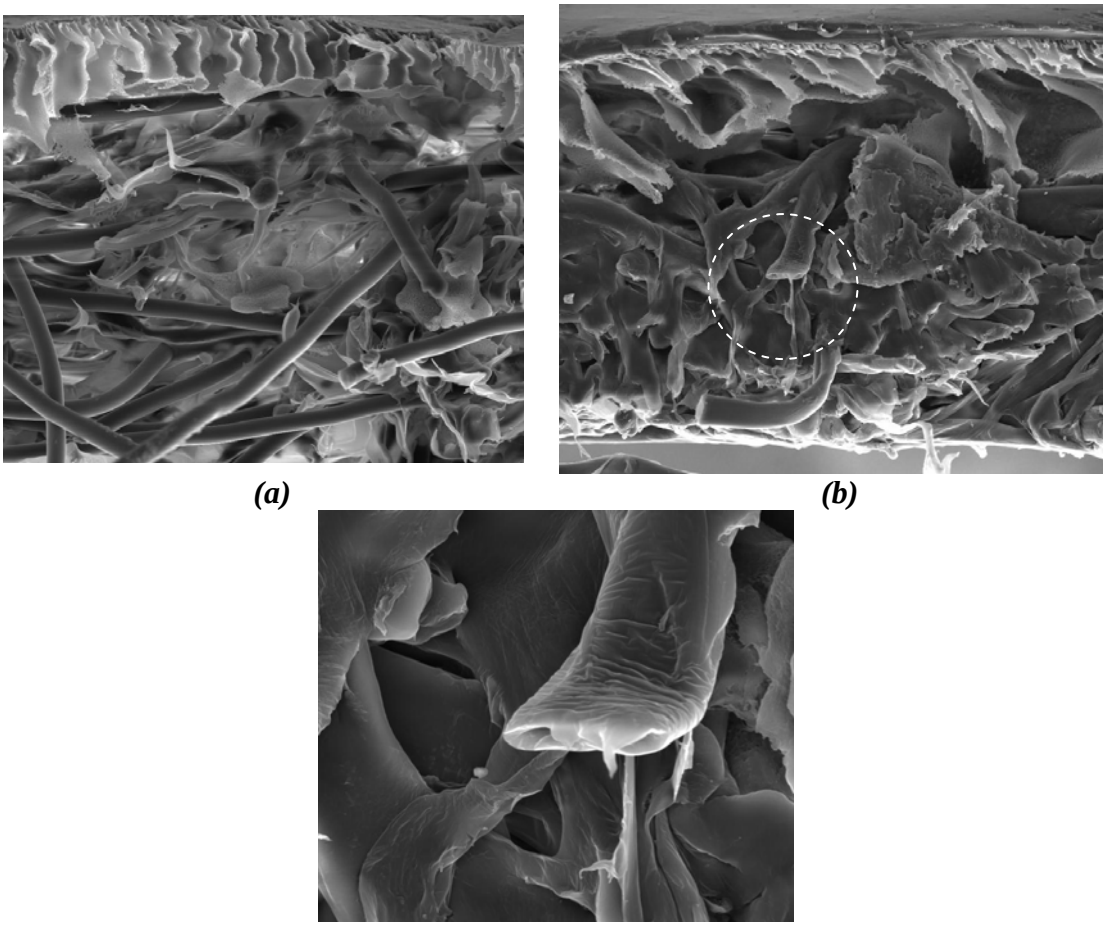

Figure 9. *Cross-sectional microscopy images of 20kDa PES membrane (a) unused membrane (1000xmagnification) and (b) membrane fouled by UF of 1.5 g.L^{-1} KGM, (1000 x magnification),(c) enlarged view of supporting material (5000 x magnification)*

Figure 9a showing the cross-sectional view of PES 20 kDa membrane represents membrane interpore structure and membrane supporting material under the membrane surface. Both the interpore structure and supporting material were clean and with no layer on the membrane surface. Microscopy image of fouled PES 20 kDa membrane (Figure 9b) showed thick layer on the membrane surface. In addition the interpore structure was damaged and the membrane supporting material was covered by the KGM (see the enlarged view, Figure 9c).

Microscopy images (Figure 8 and Figure 9) supported explanation of Figure 4 that the flux decline in KGM ultrafiltration with 20kDa PES was due to cake layer formation. In addition, the images verified result on Hermia's model that the fouling mechanism of PES 20kDa was gel/cake layer formation.

CONCLUSION

Ultrafiltration system has been used for separation of KGM solution. The permeate flux of PES 20 kDa membrane was higher than the use of PES 10 kDa. The effect of transmembrane pressure on permeate flux using 20 kDa membrane was also investigated. It was found that the increase of pressure was not always generated higher flux since the more severe fouling was found. Analysis of Hermia's model elucidated that the fouling mechanism of PES 10 kDa and PES 20 kDa were controlled by complete blocking and cake/gel formation, respectively. This result was supported with the scanning electron microscopy images.

ACKNOWLEDGEMENT

The authors would like to express their gratitude to Diponegoro University for its financial support.

REFERENCES

1. Nishinari, K. Gao, S.: Konjac Glucomannan in: *Functional food Carbohydrates* (Editors: Biliaderis, C.G., Izydorczyk, M. S.), CRC Press, Boca Raton, **2007**, 97-125;
2. Zhang, Y-q., Xie, B-j., Gan, X.: Advance in the Applications of Konjac Glucomannans and its Derivatives, *Carbohydrate Polymers*, **2005**, **60** (1), 27-31;
3. Tatirat, O., Charoenrein, S.: Physicochemical Properties of Konjac Glucomannan Extracted from Konjac Flour by a Simple Centrifugation Procecss, *LWT-Food Science and Technology*, **2011**, **44**, 2059-2063;
4. An, N.T., Thien, D.T., Dong, N.T., Dung, P.L., Du, N.V.: Isolation and Characteristcs of Polysaccharides from Amorphophallus corrugatus in Vietnam, *Carbohydrate Polymers*, **2011**, **84**, 64-68;
5. Ohashi, S.G., Shelso, A.L., Moirano, S.L., Drinkwater, W.L.: *US Patent 6,162,906*, **2000**;
6. Wagner, J.: *Membrane Filtration Handbook Practical Tips and Hints*, 2nd edition, Osmonics Inc, **2001**, 7-9;
7. Krawczyk, H., Arkell, A., Jönsson, A-S.: Membrane performance during ultrafiltration of a high-viscosity solution containing hemicelluloses from wheat bran, *Separation and Purification Technology*, **2011**, **83**, 144-150;
8. Persson, T., Jonsson, A. S.; Isolation of Hemicelluloses by Ultrafiltration of Thermomechanical Pulp Process Water – Influence of Operating Conditions, *Chemical Engineering Research and Design*, **2010**, **88**, 1548-1554;
9. Sun, H., Qi, D., Xu, J., Juan, S., Zhe, C.: Fractination of Polysaccharides from Rapeseed by Ultrafiltration: Effect of Molecular Pore Size and Operating Conditions on the Membrane Performance, *Separation and Purification Technology*, **2011**, **80**, 670-676;
10. Xie, J-H., Shen, M-Y., Nie, S-P., Zhao, Q., Li, C., Xie, M-Y.: Separation of water-soluble polysaccharides from *Cyclocarya paliurus* by ultrafiltration process, *Carbohydrate Polymers*, **2014**, **101**, 479–483;
11. Jian, W., Sun, Y., Huang, H., Yang, Y., Peng, S., Xiong, B., Pan, T., Xu, Z., He, M., Pang, J.: Study on preparation and separation of Konjac oligosaccharides, *Carbohydrate Polymers*, **2013**, **92** (2), 1218-1224;
12. Corbatón-Báguena, M-J., Álvarez-Blanco, S., Vincent-Vela, M-C.: Fouling Mechanisms of Ultrafiltration Membranes Fouled with Whey Model Solutions, *Desalination*, **2015**, **360**, 87–96;
13. Ng, C.Y., Mohammada, A.W., Ng, L.Y., Jahim, J.M.: Membrane fouling mechanisms during ultrafiltration of skimmed coconut milk, *Journal of Food Engineering*, **2014**, **142**, 190–200;

14. Liu, H., Tang, Z., Cui, C., Sun, C., Zhu, H., Li, B., Guo, L.: Fouling mechanisms of the extract of traditional Chinese medicine in ultrafiltration, *Desalination*, **2014**, **354**, 87–96;
15. Nataraj, S., Schomäcker, R., Kraume, M., Mishra, I.M., Drews, A.: Analyses of polysaccharide fouling mechanisms during crossflow membrane filtration, *Journal of Membrane Science*, **2008**, **308**, 152–161;
16. Hermia, J.: Constant Pressure Blocking Filtration Law: Application to Power Law Non-Newtonian Fluids, *Trans. Ind. Chem. Eng*., **1982**, **60**, 183-187;
17. Vela, M.C.V., Blanco, S.A., Gracia, J.L., Rodriguez, E.B.: Analysis of Membrane Pore Blocking Models Applied to the Ultrafiltration of PEG, *Separation and Purification Technology*, **2008**, **62**, 489-498;
18. Amin, I.N.H.M., Mohammad, A.W., Markom, M., Peng, L.C., Hilal, N.: Analysis of Deposition Mechanism during Ultrafiltration of Glycerin-rich solution, *Desalination*, **2010**, **261**, 313-320;
19. Kohyama, K., Sano, Y., Nishinari, K.: A mixed system composed of different molecular weights konjac glucomannan and κ-carrageenan. II. Molecular weight dependence of viscoelasticity and thermal properties, *Food Hydrocolloids*, **1996**, **10**, 229-238.
20. Montane, D., Nabarlatz, D., Torras, C., Garcia-Valls, R.: Purification of xylo-oligosaccharides from Almond Shells by Ultrafiltration, *Separation Technology*, **2007**, **53**, 235-243;
21. Mulder, M.: *Basic Principles of Membrane Technology*, 2nd edition, Kluwer Academic Publisher, Dordrecht, **1996**, 416-464;
22. Wan, Y., Prudente, A., Sathivel, S.: Purification of Soluble Rice Bran using Ultrafiltration Technology, *LWT Food Science and Technology*, **2012**, **46**, 574-579;
23. Wang, C., Li, Q., Tang, H., Yan, D., Zhou, W., Xing, J., Wan, Y.: Membrane Fouling Mechanism in Ultrafiltration of Succinic Acid Fermentation Broth, *Bioresource Technology*, **2012**, **16**, 366-371;
24. Susanto, H., Widiasa, I.N.: Ultrafiltration Fouling of Amylose Solution: Behaviour, Characterization and Mechanism, *Journal of Food Engineering*, **2009**, **95**, 423-431;
25. Hu, X., Bekassy-Molnar, E., Koris, A.: Study of modelling transmembrane pressure and Gel Resistance in Ultrafiltration of Oily Emulsion, *Desalination*, **2004**, **163**, 355-360;
26. Lo, Y.M., Yang, S.T., Minh, D.B.: Kinetic and Feasibility Studies on Ultrafiltration of Viscous Xanthan Gum Fermentation Broth, *Journal of Membrane Science*, **1996**, **117**, 237-249;
27. Jonsson A.S.: Influence of Shear Rate on the Flux during Ultrafiltration of Colloidal Substances, *Journal of Membrane Science*, **1993**, **79**, 93-99;
28. García-Molina, V., Lyko, S., Esplugas, S., Wintgens, Th., Melin, Th.: Ultrafiltration of aqueous solutions containing organic polymers, *Desalination*, **2006**, **189**, 110-118.